IIETA International Information and Engineering Technology Association
Advancing the World of Information and Engineering

Journal Européen des Systèmes Automatisés
Vol. 59, No. 3, March, 2026, pp. 797-813
Journal homepage: http://iieta.org/journals/jesa

Optimization of Shock Absorber Performance Under Controlled Compression Angles: A Study on Structural Integrity and Fatigue Life

Auday Shaker Hadi[1*], Ahmed Hashim Kareem[2], Bassam Ali Ahmed[3], Malik N. Hawas[4], Hasan Shakir Majdi[5]

[1] Mechanical Engineering College, University of Technology- Iraq, Baghdad 10001, Iraq
[2] Mechanical Techniques Department, Amarah Technical Institute, Southern Technical University, Basra 44001, Iraq
[3] Electromechanical Engineering College, University of Technology- Iraq, Baghdad 10001, Iraq
[4] Power Mechanic Engineering Department, Dean of the Technical Institute in Al-Musayyab, Al-Furat Al-Awsat Technical University, Kufa 54001, Iraq
[5] Department of Chemical Engineering and Petroleum Industries, Al-Mustaqbal University College, Hillah 51001, Babylon, Iraq

Corresponding Author Email: Auday.S.Hadi@uotechnology.edu.iq

https://doi.org/10.18280/jesa.590322

Received: 4 January 2026
Revised: 1 March 2026
Accepted: 11 March 2026
Available online: 31 March 2026

Keywords:
compression force angle, fatigue life analysis, vibrational response, ANSYS modal analysis, shock absorber design

ABSTRACT

The research study investigates the influence that compression force angles produce on the nature of shock absorber operation in relation to structural integrity and vibration, in addition to wear life. To compare the various absorbers, the study focuses on Analytical System (ANSYS) simulations in which the compression angle is set at 90°, 45°, and 30°. The results have underscored the significance of such angles to deformation, reaction, vibrational and fatigue strength. A 90° absorber will have low deformation, and is appropriate because reaction forces will be balanced, thus adding structural stability and fatigue life. Conversely, the absorbers with 45° and 30° angles develop more deformation, imbalanced forces, reduced fatigue life because of a lesser axial force component, and reduced lateral stresses on steeper inclinations. The preventability of vibrations reduces with a decrease in the angle, as indicated by modal analysis, and further exacerbates performance. These findings emphasize the need to maintain a perpendicular compression angle to improve the stability and integrity of the shock absorber design. The article has the potential to fill the knowledge gap in the optimization of absorber geometry and forces orientation, particularly when forces are not close and orthogonal, like in automotive and heavy-duty systems. It would also provide useful suggestions for designing high-performance absorbers at different operating conditions.

1. INTRODUCTION

Shock absorbers play a significant role in a mechanical system. In the automotive, aerospace, and heavy machinery sectors, shock absorbers serve as the primary means of vibration isolation and energy absorption. The safety and longevity of automobiles are essential components of automotive life. The carrying capacity and material characteristics have, with few exceptions, remained the main focus in traditional shock-absorber design, resulting in relatively unexplored research on how compression-force angles affect performance shape. The direction of compressive forces significantly influences fatigue's strength and characteristics. When compression loads are not mutually perpendicular to the primary load, the effective axial load decreases, thereby increasing deformation and the unequal distribution of forces, which increases stress concentrations at local positions. The effects are spread under the assumption that they become more relevant under realistic operating conditions, where the shock absorbers are subjected to complex, dynamic loading. The manuscript tries to fill the gap in knowledge related to the compression angle, deformation, reaction forces, vibration stability, and fatigue resistance. The lessons learned are priceless in building shock-absorber injection practice, especially where shock absorbers would find application in non-uniaxial forces.

Purnomo et al. [1] calculated both the stresses and safety component losses due to cyclic loading in shock absorbers and the losses in the finite element analysis. Simulation demonstrated the accumulation of repeated forces on the stress in a certain area, compromising structural safety margins. Tekeci and Yildirim's [2] contribution was creative in applying fatigue frequency-domain analysis to the rigorous vibration testing conducted in the laboratory's empirical section. The researchers ensured a very robust case for predicting premature component failure under dynamic physical loads. Tang et al. [3] examined the high-cycle fatigue behavior of landing gear structures using a practical application of advanced finite element models that account for the control-variable shock absorber travel parameters. Their analysis

demonstrates the existence of a critical level of stress intensities that are grossly deteriorated under matching dynamic load conditions, through analysis of quasi-static load distributions at various positions of the stokes. Liu et al. [4] explored a method for measuring the relationship between the cross-sectional excitation deflection angle and mitigation, investigating the effect of varying excitation deflection angle on mitigation using the vibro-mechanical properties of variable cross-sectional metal rubber isolators. Kiranet al. [5] have developed an ANSYS computational environment by conducting a systematic examination and optimization of the structural design parameters of automotive shock absorbers. Their experimentation established a unique way of establishing critical locations of potential mechanical breakdown by identifying equal stresses and breaking tensile strength. Kumhar [6] aimed to understand the structural integrity and bouncing behavior of springs in motorcycle shock absorbers through a finite element analysis case study of the component's response under applied loads. The researchers found that induced mechanical stress and deformation are significantly reduced by an orderly change in the spring's coil diameter. Li et al. [7] conducted detailed finite element modal analysis and empirical testing, including physical testing, to determine how compression devices in farm combine harvesters may resonate. Using ANSYS-Workbench to create computations and compare the modal parameters obtained with testing using a dynamic impulse hammer. Zhang et al. [8] developed a detailed, dynamic computational model to predict the fatigue life of the suspenders of an arch bridge by forecasting the dynamic spectra of distress caused by the loads from local moving vehicles. Through the combination of Monte Carlo traffic flow simulation and the use of the finite element stress analysis. Adam et al. [9] proposed a stochastic modeling approach to evaluate the strain-based fatigue reliability of automobile lower-arm suspensions under variable road conditions, effectively overcoming the constraint imposed by limited experimental load-time histories. It uses the count of rain-flow cycles in synthetically generated strain signals. In Zhang et al.'s study [10], the fatigue resistance of motor hangers in high-speed electric multiple units was investigated, and constant-torque ripples and reduced weld penetration were found to drastically increase localized structural stresses. In a finite element study together with vigorous field tests, their study showed that the near-resonance conditions largely play a role in boosting the dynamic deformation at the welded joints, and thus, offer cracking fatigue a solid driving force for the advancements. Pan et al. [11] have proposed a novel two-dimensional Intelligent Driver Model that can be applied to traditional traffic load models, using real-world traffic road-vehicle path information and crosswalk traffic on bridge decks. By carrying out a comparative research of a long-span suspension bridge. By incorporating transient thermal variables associated with varying vehicle loads into the ANSYS computational platform, Xiao et al. [12] advanced the investigation of fatigue life in the welds of the steel deck of the suspension bridge. They discovered that one factor that can determine the calculated equivalent stress of vulnerable joints in the U-rib structure is temperature gradients. Dai et al. [13] studied the structures, integrity, and mechanics of carbon fiber-reinforced polymer composite helical springs (CFRP) at various non-axial compression angles. The test showed that multi-axis loading arrangements cause deep-seated changes in stress components and the behavior of stiffness and strain in complex composite suspensions of the parts. The predictive scheme for fatigue life and structural durability of hydraulic shock absorbers introduced by Czop and Wszolek [14] is holistic and model-based. The report found that the mechanical strength of highly stressed-out valve assemblies is a significant predictor of the overall performance and service life of fluid-damping systems. The literature reviewed provides a good summary of current trends in research on the behavior of spring-damper structures subjected to vibrational and fatigue loading. Though tremendous improvements have been achieved, especially in the use of ANSYS Workbench for simulation and assessment, obstacles in modeling complex loading cases and material behavior remain. The gaps mentioned should be addressed in future research as well; however, greater attention should be paid to verifying other gaps through experiments, and more advanced computational frameworks should be developed. Tilting of the troops instead of making the direction perpendicular will minimize the axial element, hence augmenting deformation and ensuing sideways strains. This process can hasten fatigue failure and reduce the device's service life. Interestingly, when a shock absorber is often loaded or overstrained non-perpendicularly, e.g., in off-road vehicles, heavy equipment, and in maneuvers with sharp turns or steep elevations. One of the premises underlying the present-day research issue is the nature of the compression force angle of shock absorbers, as it is hypothesized that this angle fundamentally affects the life of shock absorbers. Specifically, a load applied at angles other than 90° is expected to cause increased deformation, unequal force distribution, and a resulting shorter fatigue life. To that end, the guiding study question is: What is the effect of the compression-force angle of shock absorbers on their structural integrity, deformation, vibration, and fatigue life under cyclic loading?

2. METHODOLOGY

The shock absorbers simulation process starts in the SolidWorks design area, where the operating shock absorber is modeled, as shown in Figure 1. The layout is converted to a step format and exported to ANSYS before computation. The three stages of the FEA process, including pre-processing, analysis, and post-processing, are followed by result evaluation. Boundary conditions and structural version modeling have also been employed. Mesh grid independence and convergence tests determine the ideal model optimization and appropriate mesh size. The findings demonstrated that the fatigue cyclic loading response shape consisted of stress, deformation, and safety components. The ANSYS program displays the stress distribution as a contour plot.

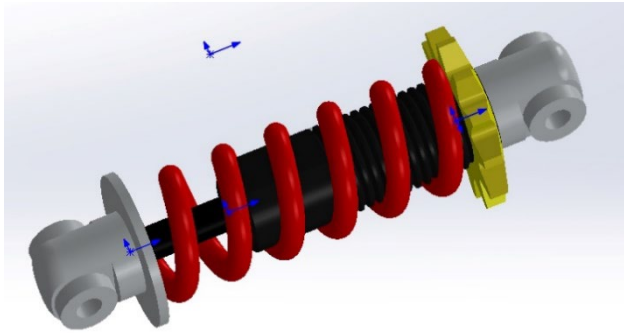

Figure 1. Shock absorber SolidWorks design

Various applications, such as business equipment operating under variable loading conditions and vehicles shifting on difficult roads, may exhibit random vibrations. Vibration levels will no longer be readily foreseeable in light of those cases. One characteristic of random vibrations is the absence of periodicity [15], as seen in Figure 1. Six effective motion combinations can fully characterize solid oscillatory motion: three rotating axes (0x, 0y, 0z) and three translational directions (x, y, z). These six additive components can break down any complex body action. As a result, it has been said that these bodies possess six degrees of freedom. The finite element method (FEM) and modal evaluation solve the system's response to a known external force [16]. As a complicated alternative, these authors will not refer to them in an elemental sense. To grasp the basics of vibration evaluation devices, however, it is most valuable to recall how forces and systems interact. Three basic principles underpin the assessment technique used in random reaction analysis [17]. Power is one characteristic used to handle vibration in random reaction analysis rather than in vibration time series. Figure 2 shows the drift chart of the simulation system.

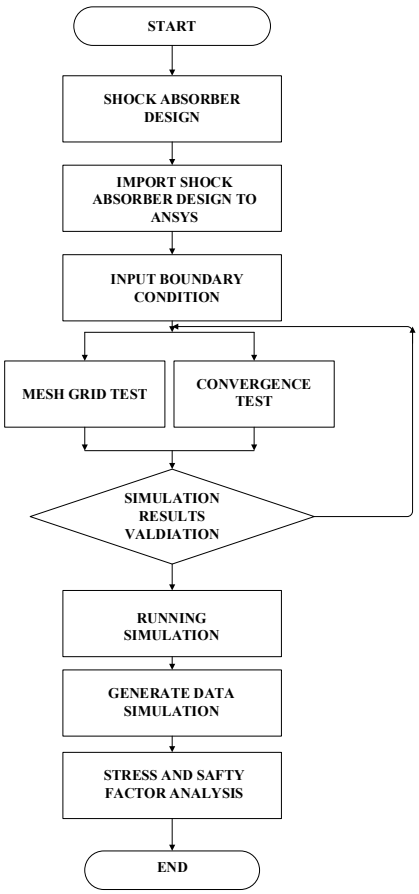

Figure 2. Simulation process procedure scheme

Random vibrations can manifest in commercial devices operated under arbitrary loading conditions and in vast package ranges, like when a car is shifting on uneven roads. The instantaneous amplitude values will, in some cases, be unpredictable. Figure 1 shows that the characteristic lack of periodicity is one of the fundamental characteristics of random vibration. Such a complex force movement can be decomposed utilising these six additive components. Accordingly, six degrees of freedom are stated for each body [18]. Then, modal analysis and the FEM are applied to predict the external effect of the system. However, studying interactions between forces and systems to understand the basic principles of vibration analysis is useful. Random response analysis divides the evaluation method into three subsequent methods.

Vibration is treated not through time, when considered for random reaction analysis, but using metrics like the preferred deviation and energy spectral density function (PSD). A few standards state that a PSD response acceleration level must satisfy Standard [19] to be considered in vibration analyses. Following the guidelines for defining and quantifying the mechanical vibrations' equilibrium point, or maximum amplitude (peak). The difference between the highest and lowest peaks is called the "swipe" (peak-peak). Because temporal consciousness is symmetrical in this situation, the span of a sinusoidal oscillation is exactly twice the peak amplitude [20]. Minor rules from strain standard deviation (RMS stress) utilisation obtained via random response analysis are used to assess the tiredness lifestyle. There are numerous other ways for fatigue analysis, though 1σ, 2σ, and 3σ stress values are simple to use [21]. Consequently, data processing is one of the most important steps in the prognostic process. Amplitude and time resolution must be adequate for collector vibration sensors [22].

2.1 Material assignment and ANSYS conditions

The SolidWorks software program shock absorber design is shown in Figure 1. Absorber shock manufacturing data and experimental testing defined the model materials. The material details of the shock absorber spring are presented in Table 1. The ANSYS simulation model assumed frictional contact between the additives in the piston rod and inner tube and between the spring ends from the nut and the internal tube facets. Fourth contact between the nut and the outer piston teeth is constant as a bounded contact. Contact information is shown in Figure 3. The ANSYS model boundary conditions were as follows: For the fixed support, the shock absorber was tied down to a fixed boundary at one end, thus keeping the spring at its position during the simulation. This arrangement simulates a stationary attachment of the shock absorber in a mechanical setup. The working load was shown through the compressive force of 1200 N acting on the lower part of the shock absorber, and the upper part of the shock absorber was clamped, indicating the typical arrangement corresponding to the standard form in which the upper terminal of the shock absorber is clamped at the vehicle or the structural framework. The compression angles of force to be applied were set to 90°, 45°, and 30° to explore the effects of different angles on deformation, stress distribution, and fatigue life. They loaded the shock absorber cyclically at the chosen compression angles. This simulation replicates the cyclical kinetics that shock absorbers experience during daily vehicle and machine operation cycles. The cyclic loading was done through random response analysis using a predetermined loading history. Stress, deformation, and safety factors were assessed considering the load cycles, thereby evaluating the impact of cyclic loading on these factors. The fatigue life evaluation was conducted based on the minor principal stress values obtained from the simulation results. The analyses were performed using ANSYS Workbench, a powerful structural/fatigue analysis software. A recent software version conducted a detailed finite element analysis (FEA) and random vibration analysis. The first deformation and reaction force analysis was

performed using static structural solvers, whereas the fatigue life of the shock absorber under cyclic loading was evaluated using transient structural solvers. Natural frequencies were obtained through a modal analysis, while a random vibration solver was used to estimate the system's reaction to variable excitations.

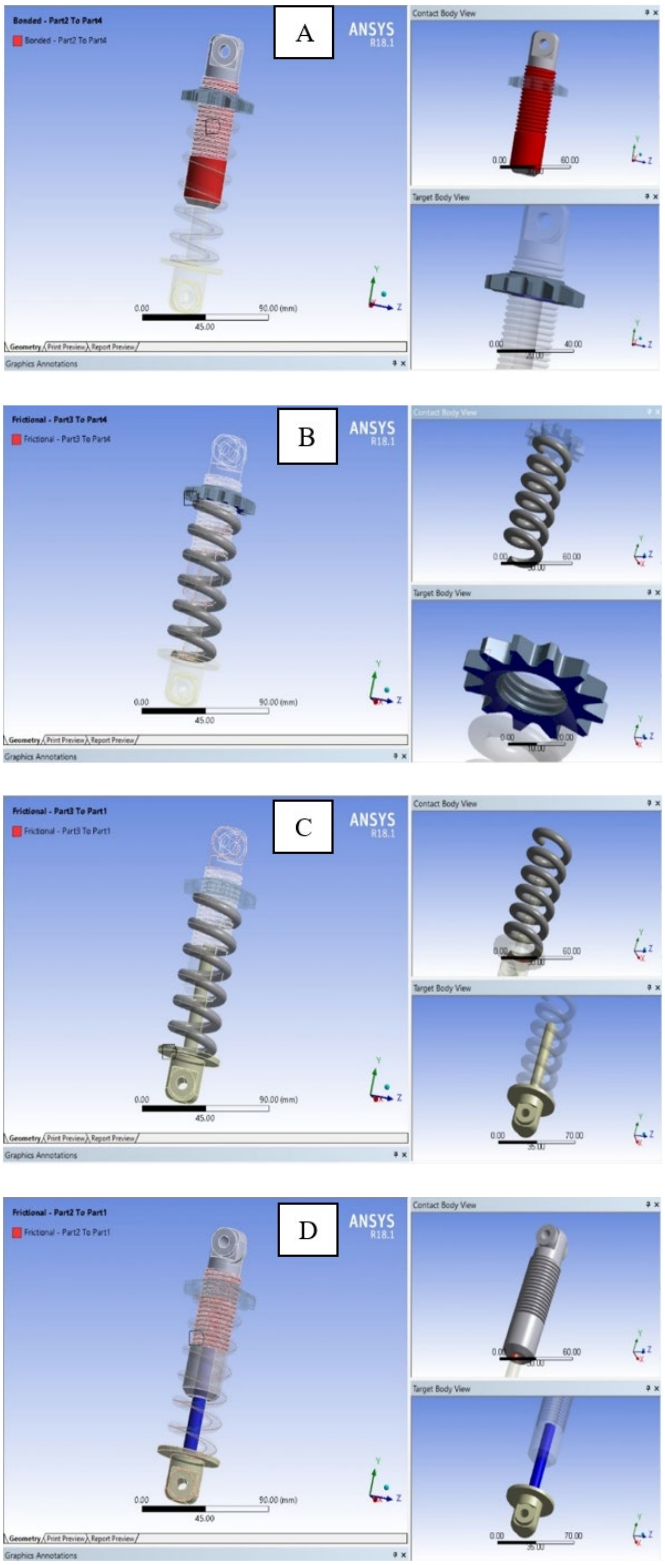

Figure 3. Simulation model contact points are defined. (A) Between the nut and the piston part (B) and (C) for the sp, ring two ends, and (D) between the inner tube and the piston

Table 1. Shock absorber material properties [23]

Parameters	Value
Material	Low-carbon steel
Mass per wheel (m)	62.5 kg
Density	7.833e-06 kg/mm³
Young modulus	2.0555e+05 MPa
Tensile yield strength	1595 MPa
Stiffness coefficient (k)	1.73

2.2 Mathematical equations

To calculate the displacement cost due to compression pressure, authors typically apply the principles of mechanics and recall the precise conditions of material type, structural properties, and loading conditions. Here's a popular technique, assuming you're working with a linear device (e.g., a spring, a beam, or another elastic system). For the reason of figuring out the connection between pressure and displacement for most linear elastic substances, Hooke's Law offers a trustworthy relationship [24]:

$$F = K \times x \tag{1}$$

F is the reaction force, k is the stiffness or spring constant (measured in force per unit displacement, N/m), and x is the displacement (mm). The bodily traits of the surprise absorber spring, along with twine diameter, coil diameter, quantity of lively coils, and cloth houses, can be used to determine the surprise absorber spring stiffness consistent with the following formula for a helical compression spring [25]:

$$K = \frac{Gd^4}{8ND^3} \tag{2}$$

where, G is the shear modulus of the spring fabric (N/m²), d is the diameter of the wire (m), and D is the implied coil diameter (distance from the middle of the cord on one side of the coil to the middle on the opposite side, in meters), N is the number of live coils. This method is accurate for springs with acknowledged specs and allows you to calculate okay without physical testing. To calculate the equal (or von Mises) stress in a shock absorber spring from the displacement, the connection among displacement, pressure, and stress in the spring must be understood. For a helical compression spring, the primary pressure under axial load is shear within the spring cord. The usage of the equation may calculate the maximum shear stress (τ) within the spring wire [26]:

$$\tau = K_w \frac{8FD}{\pi d^3} \tag{3}$$

where, K_w is Wahl correction factor, F is the force calculated from Hooke's Law, D is the mean coil diameter of the spring (distance between the centers of the wire on opposite facets of the coil), and d is the diameter of the spring cord, to discover the equivalent (von Mises) pressure σ_{vm}, which money owed for mixed stresses, the most shear pressure is calculated using the following equation [27]:

$$\sigma_{vm} = \sqrt{3}\,\tau \tag{4}$$

Substituting τ from the shear stress formula:

$$\sigma_{vm} = \sqrt{3}\,\frac{8FD}{\pi d^3} \quad (5)$$

Perform modal analysis to find the system frequency. Perform random vibration analysis with modal analysis used as the initial condition, with PSD Base Excitation implemented within the preferred course. Evaluate stresses and deformations at (1) sigma values. A 1200 N compressed force was applied to the shock absorber's lower part for the three-angle vibration analysis. The upper part of the shock absorber serves as constant support for the alternative side, as illustrated in Figure 4.

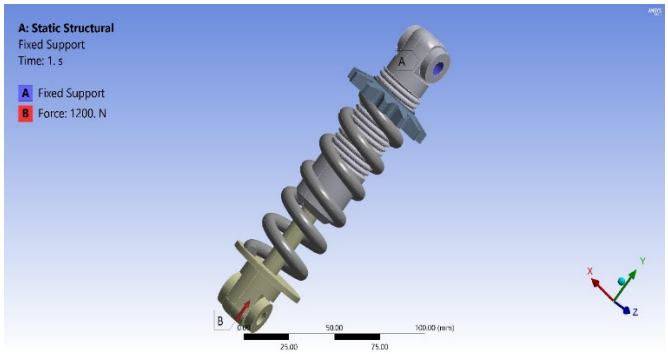

Figure 4. Applied force and fixture

To examine the effect of a force on the vibration and fatigue resistance of the shocked observer, the implemented pressure was subjected to 90°, 45°, and 30° stages by controlling the shock absorber perspective, as shown in Figure 5. All the following calculations determine the pleasant mesh characterised by the surprise absorber state of affairs at 90°.

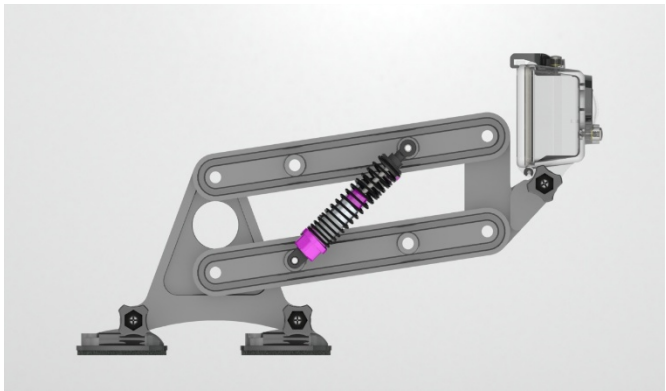

Figure 5. Fixture and applied force angle control in the structure

2.3 Mesh analysis and validation method

The above examination method was applied due to increased structural complexity for shock absorbers. At the centre of FEM was the relationship between the assembled stiffness matrix, which related force and displacement fields throughout the elastic domain. A finite detail discretisation system computed stress and strain using the strain-displacement relationship [28]. Meshing was changed to control the reuse of international and local mesh sizes. Mesh inflation was set up with a swap and the ratio of 0.272. When selecting the type and size of the mesh for the simulation, consider the mesh independence study. This test was defined using the mesh grid [29, 30]. The impact of the independence test for diverse mesh sizes is confirmed in Table 2. Furthermore, the choice of grid mesh length is depicted in Figure 6(A), ranging from 3.25 mm to 2.0 mm with a price increment of 0.25 mm. Reducing or increasing the mesh length negatively impacts the simulation run time; hence, the grid independence test is an appropriate tool for validating simulation pre-processing. Generally, as long as these effects remain strong, the grid mesh parameter is considered sufficient. Deformation adjustments therefore spanned a 10.9% to 6.1% reduction, and mesh adjustments ranged from 10 to 4.5 mm. On the other hand, the variant in most pressure tiers is gradual. Applying 5.0 mm as the mesh size, each deformation limit and the majority of stresses coalesced, and therefore, the mesh size of 5.0 mm was chosen.

Table 2. Mesh independence

Mesh Size	Nodes	Elements	Max Deformation	Max Stress
10 mm	14733	7508	0.0397	96.97
9.5 mm	14855	7560	0.0374	97.02
9 mm	15546	7970	0.0333	97.05
8.5 mm	15571	7923	0.0293	97.09
8 mm	16607	8533	0.0289	97.11
7.5 mm	16868	8647	0.0274	97.18
7 mm	17618	8950	0.0263	97.23
6.5 mm	18682	9550	0.0227	97.27
6 mm	19410	10060	0.0241	97.32
5.5 mm	21765	11385	0.0231	97.38
5 mm	24906	13160	0.0198	97.42
4.5 mm	30530	16438	0.0197	97.42

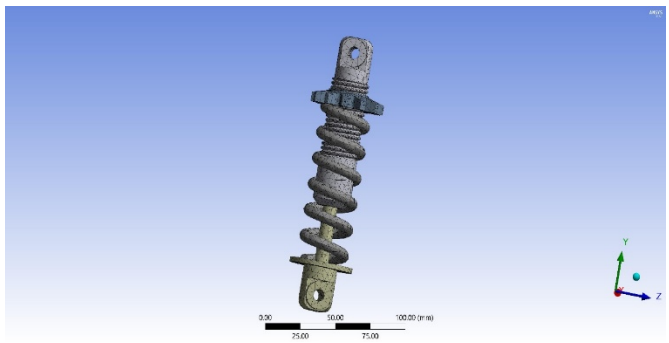

(A)

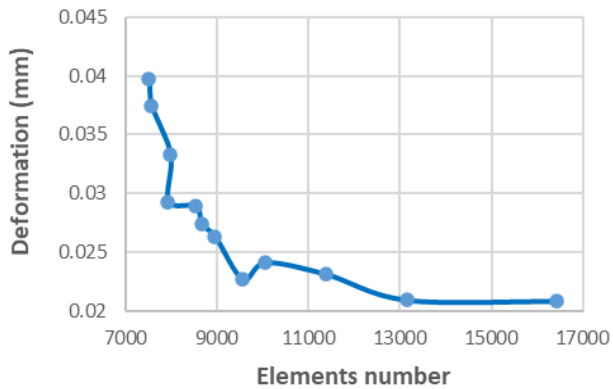

(B)

Figure 6. (A) ANSYS model meshing, (B) Deformation convergence graph

In addition to the mesh independence test, a mesh convergence test was conducted to verify the simulation's

accuracy, as shown in Figure 6(B). Different mesh densities were chosen for a particular position of the shock absorber to determine the solution. The results were then compared to determine the difference between successive mesh sizes. The meshing process was performed for a range of meshes from 10 to 4.5 mm to achieve the deformation of the modelled tooth surfaces. Kushwah et al. [31] stated that mesh convergence was possible when the percentage difference in deformations was less than 1%. Another consequence was that a 5.0 mm mesh size has a deviation of 0.02%, which is accurate enough to be used.

2.3.1 Validation

Wakchaure et al. [32] investigated the effect of mesh density on the accuracy and performance of surprise absorber simulations in ANSYS. They determined that adaptive meshing, which dynamically adjusts the mesh density in regions of high stress or pressure, notably improved the accuracy of outcomes, particularly in complex impact situations. This was validated through numerical simulations and experimental checks, ensuring that the chosen mesh configuration is efficient and reliable.

Similarly, Silva et al. [33] extensively reviewed different mesh refinement strategies during the numerical modelling of shock-absorbing structures. They noted that testing a high-quality mesh in critical areas, such as the interface at contact points and near errors, can produce significantly higher-quality outputs of the computed results. However, they emphasised the need to enforce a moderate tradeoff between computation cost and model performance. An extremely complicated mesh, which would not yield equally significant accuracy improvements, would be very costly to implement. The validation process they followed in the study involved comparing the simulation sonnets with the experimental readings, thereby supporting the idea that a sensible mesh background cannot be overlooked in accurately predicting the general behavior of shock rumbling devices.

2.4 Vibration amplitude measurement

Vibration analysis and engineering: Vibrations of a mechanical system, including shock absorbers, cannot be accurately rated or measured solely by appearance without correctly quantifying vibration amplitude. Shock absorbers are designed to reduce vibration and minimize the transfer of kinetic energy between the road and the chassis or body of a vehicle. The important concepts of vibration (maximum amplitude (peak)) and sweep (peak-to-peak) amplitude are used in order to evaluate their performance [5]. The outcomes of these measurements provide insight into the operation of shock absorbers under different operating conditions and loads. The highest amplitude or the highest absolute vibrating motion about the equilibrium position of the vibrating system of the machine, which is frequently called the largest amplitude or even the largest amplitude [34]. This is either positive or negative, calculated relative to the equilibrium or rest position of the shock absorber. For example, in a sinusoidal waveform, a common representation of oscillatory motion, this peak amplitude corresponds to the apex of the wave crest or trough. Since shock absorbers operate in dynamic environments, maximum amplitude measurement allows engineers to identify the extreme points of oscillation induced by road impacts, thereby assessing the absorber's efficiency in mitigating large displacements [35]. Peak amplitude is particularly relevant in cases where non-linearities or transient effects influence system dynamics. In mechanical systems with excessive vibration amplitudes, such as poorly damped shock absorbers, high peak amplitudes may indicate potential mechanical failure or component fatigue over time [36].

2.5 Fatigue strength evaluation

Fatigue life is classified by minor policies derived from the same old stress standard (RMS stress) received through random response evaluation. Multiple methodologies exist in fatigue evaluation, but utilising 1σ, 2σ, and 3σ stress values is simple. Data processing includes supplying information, extraneous noise, irrelevant alerts, and indicators shown in a suitable format for diagnostic purposes. Consequently, data processing is a critical step within the diagnostic procedure [37]. Data from vibration sensors ought to have enough resolution in each amplitude and temporal dimension. If the information received is digital, the tool's bit depth must be excessive enough to make certain vital amplitude decisions. High decision gadgets offer evaluation with more suitable precision, but they may be dearer and demand advanced performance specifications.

2.6 Simulation parameters summarized

The finite element simulations were performed using ANSYS Workbench, with a Structural Static solver (ANSYS Structural) used for modeling deformation and reaction forces [28], a modal analysis (ANSYS Modal) for obtaining the natural frequencies, a random vibration solver in order to obtain the vibrational response, and a transient structural solver (ANSYS Transient Structural) for estimating the fatigue life under cyclic loading. Import of the shock absorber model in the STEP format from SolidWorks.

Details of mesh independence and convergence are discussed in a separate publication, demonstrating that mesh sizes with the element sizes of 10 mm and 8 mm generally yield the same mechanical response as with smaller mesh sizes of 7 mm, 6 mm, and 5 mm. The final selected size for the global mesh was 5.0 mm, a compromise between accuracy and computational cost, resulting in 24,906 nodes and 13,160 elements. Inflation layers with a growth ratio of 0.272 were implemented close to contact areas to resolve stress gradients accurately.

Boundary conditions were defined as fixing the eyes of the shock absorber at the top end to simulate the mounting point, and a compressive load was applied to the bottom portion of the shock absorber (1,200 N at 90° to the shock absorber axis, 1,200 N at 45° to the shock absorber axis, and 1,200 N at 30° to the shock absorber axis). The contact between the nut and piston was assumed as bonded, while frictional contact was defined between the piston rod and inner tube and the spring ends with adjacent components. The cyclic loading was realized by subjecting a sequence of random wind speeds, similar to what would be experienced in real operational conditions, through a predefined loading history.

The fatigue life modeling in the present study adopts von Mises equivalent stress as the fatigue damage parameter, which accounts for all three components of multiaxial stresses, which are later combined, and is applicable to ductile materials such as the low-carbon steel spring material considered in this work [28]. This technique is computationally efficient by

reducing complex stress states to a scalar, and it is convenient, especially compared to conventional techniques for estimating fatigue life. Another assumption made by the model is that the material in the parts of a shock absorber is homogeneous and isotropic, so that mechanical properties (Young's modulus, yield strength) are independent of location throughout the shock absorber. The assumption is that material behavior is universal and that no local variation in properties exists, since such variations may be due to manufacturing errors, microstructural differences, or time-related degradation, which can influence fatigue strength in real-life scenarios.

Finally, it assumes linear-elastic behavior under cyclic loading, ignoring possible nonlinear or time-dependent phenomena (plasticity, creep, microstructural evolution). Input from transient structural analysis will then be used for fatigue in the form of minor principal stresses, alongside changes such as fixed boundary conditions and a more idealized angle of load, all of which reduce simulation accuracy.

3. RESULTS AND DISCUSSION

3.1 Deformation

The deformation process is based on viscoelastic phenomena, a standard concept in material science. The shock absorber deformed due to the compressive force on point (B) in Figure 4. Two force cases with angles of 45° and 30° were analyzed for two compounds in two directions, and the results were input into ANSYS to calculate the effects of the three angles on deformation, stress, vibration, and fatigue. Figure 7 shows the deformation amount of the shock absorber according to the applied force without vibration for the three cases, respectively. The magnitude and throatiness of compressive forces are the dominant factors in the deformation of shock absorbers. With this kind of force being collocated with the axis of the absorber, the deformation subsequently achieved has a direct correlation with both the extreme of the applied load and the spring's rigidity. The compression angle decreases, transforming to 90°, then to 45°, and finally to 30°, where the force distribution through space varies, manifesting a visible deformation escalation.

Table 3 shows the deformation value due to the 1200 N applied force compound in the three selected angles. The maximum deformation recorded was 1.890 mm when the shock absorber worked at a 30° angle. In comparison, with deformation values of 90° and 45° angles, the effects of the force applied angle can be demonstrated.

Table 3. Shock absorber deformation according to the compression force angle

Force Applied Angle	Maximum Deformation (mm)
90°	0.019
45°	1.550
30°	1.890

The shock absorber spring deformation increases when the applied compression force angle decreases from 90° (perpendicular) to 45° and then to 30° because the effective component of the force acting along the spring's axis decreases with the angle. When a force is applied at an angle, only a portion of that force contributes directly to the spring's compression (axial deformation). When a force F is applied at an angle θ to the spring's axis, only the force component along the spring's axis contributes to the spring's compression. The following equation gives this component:

$$F_{effective} = F \times \cos\theta \tag{6}$$

where, F is the applied force, θ is the angle of the force relative to the perpendicular (axial) direction of the spring. As the angle decreases from 90° to 45° and then to 30°, the cosine of the angle increases, making the effective force along the spring's axis smaller. Since the deformation (x) of the spring is directly related to the effective force along its axis by Hooke's Law, according to the following equation:

$$X = \frac{F_{effective}}{K} = \frac{F\cos\theta}{K} \tag{7}$$

A decrease in cos (θ) (as the angle θ decreases) leads to a larger deformation x. To break this down: At 90°: When the force is applied directly along the spring's axis (θ = 90°), cos (90∘) = 1, so:

$$F_{effective} = F \tag{8}$$

This angle produces the maximum possible effective force along the spring axis, resulting in the minimum deformation required for a given force. With a 45° angle, cos (45∘) ≈ 0.707, so the effective force along the spring's (x) axis and (Y) axis is:

$$F_{effective} = F \times 0.707 \tag{9}$$

Now, only about 70.7% of the original force contributes to axial compression, requiring a greater deformation to achieve the same level of force along the spring's axis. When the angle further decreases to 30°, cos (30°) ≈ 0.866 and sin (30°) ≈ 0.5, so:

$$F(X)_{effective} = F \times 0.866 \tag{10}$$

$$F(Y)_{effective} = F \times 0.5 \tag{11}$$

Even less of the applied force directly compresses the spring along its axis, increasing the deformation further to balance the applied force. When the compressor angle is 90°, the force used becomes normal to the longitudinal axis of the shock absorber, thereby increasing the effective axial peak. This design facilitates uniform weight distribution along the spring, leading to minimal deformation. Experimentally, deformation at this angle was minimal, at 0.019 MPa, and proved efficient in both load transmission and minimal strain. The design implication is therefore definite: the orthogonality of forces with the spring axis maximises spring stiffness. It minimises the reduction of spring deformation in nominal loading situations. On the other hand, reducing the compression angle to 45° and then to 30° reduces the axial component of the force exerted. The force is then split into an axial and a lateral force, thus successfully lowering the force's ratio to compress the spring along the axial axis. When the angle becomes smaller, the proportion of the total force used to induce axial compression will decrease; at 45°, about 70.7% of the force will go into axial deformation along the lines of the cosine relationship, but at 30°, the contribution of axial deformation will be further reduced. Based on this, to achieve the same

compression, the spring will, in turn, have to experience more deformation to offset the lost axial component.

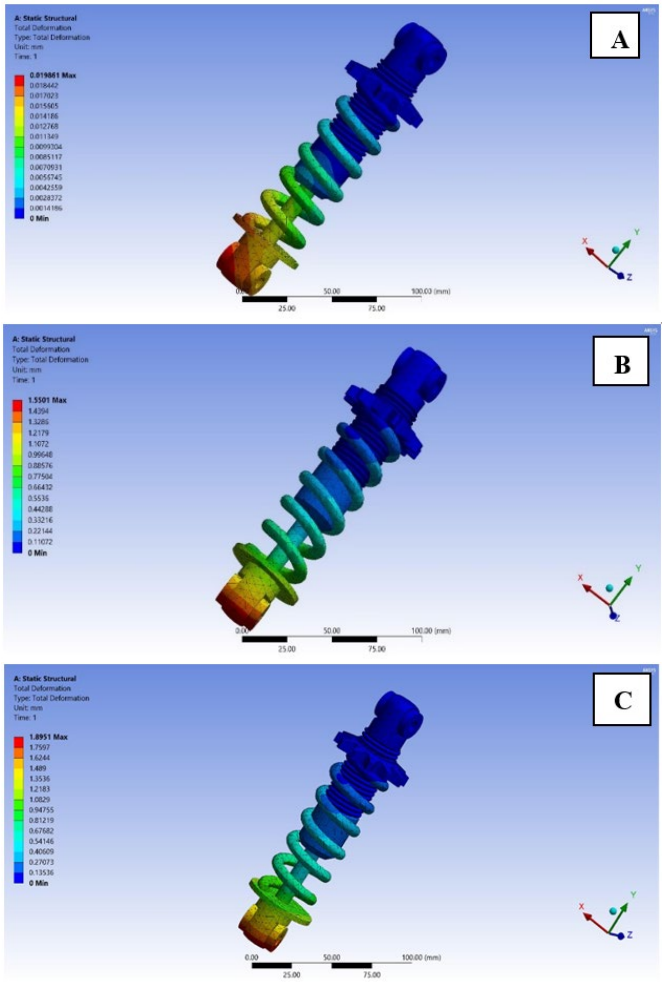

Figure 7. The deformation of the shock absorber according to the force applied angle without vibration (A) 90°, (B) 45°, and (C) 30°

To maintain the desired compression, the springs' deformation must increase further to offset the reduced axial force. With a 90° orientation bonus, the absorber design must contend with increased deformation, which is 1.550 mm at 45° and 1.890 mm at 30°. The overlying deformation at lower angles is explained by a relative reduction in axial loading and the generation of lateral components. These lateral forces act less sensitively on the spring action, produce shear and bending forces, and magnify the actual distortion. The absorber's resulting physical behaviors include increased lateral displacement and strain, leading to fatigue damage over the long term. In terms of design, those findings point to the need to maintain 90° alignment in applications requiring structural rigidity and low deformation. When non-perpetual loading cannot be avoided, e.g., in applications involving off-road vehicles or equipment that experiences dynamic stress, the absorber's shortcomings should be sized to account for the resulting increase in deformation. In that manner, incorporating fortified materials, custom geometry, or extra-damping mechanisms can become an absolute necessity for dampening the destructive effects of lateral forces. In conclusion, the smaller the compression angle, the greater the deformation, since a smaller portion of the applied force is directed toward compressive motion of the axle, while a greater portion is exerted laterally, resulting in greater stress on the shock absorber. This physical behavior should be considered when designing absorbers, as it plays a major role in determining durability, performance, and the amount of strengthening required to maximize performance under non-perpendicular loading conditions.

3.2 Reaction force

Shock absorbers should perform consistently across various road conditions, vehicle loads, and temperatures. By examining the reaction force, engineers can also optimize absorbers for use in specific packages, such as lightweight autos, heavy trucks, or off-road vehicles [38]. This allows special design enhancements to also withstand harsh work conditions, optimizing not just style but also toughness. In this, look at the compression pressure applied over time, assumed to be 1 second. In ANSYS, to research the response force for the investigated angles, the response force directions for the three instances were continually in contrary directions of the effective force or its compound result in line with Newton 3 law, as illustrated in Figure 8. The behavior, value, and direction of those response forces for the three selected angles are proven in Figure 9.

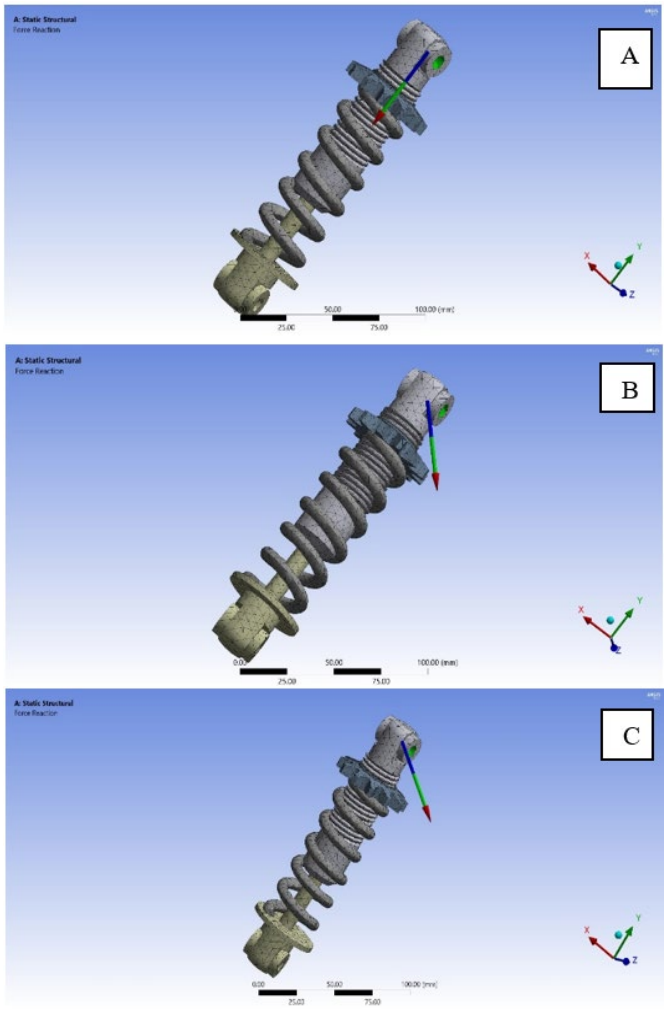

Figure 8. Reaction force direction (A) 90°, (B) 45°, and (C) 30° effective force angle

Charts in Figure 9 illustrate the behavior of the reaction force over time as a function of the compression force angle, and also display the total reaction force for the three cases.

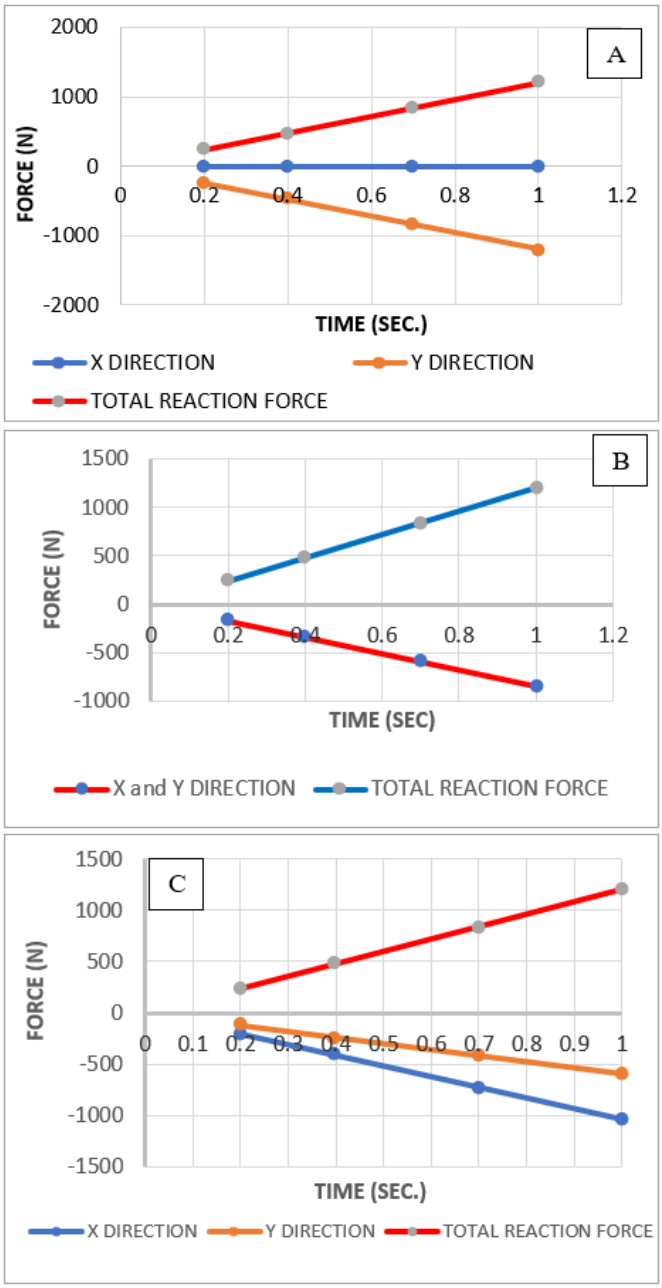

Figure 9. Reaction force compounds and behaviour according to the effective force angle. (A) 90° (B) 45°, and (C) 30°

In chart (A), where the pressure is applied perpendicularly (90°), the response force reveals a quite balanced distribution along the X and Y directions, achieving height values of around ±1500 N. This configuration represents the most pressure aspect appearing along the surprise absorber's primary axis, leading to the maximum solid and predictable reaction in terms of amplitude. The ease and high symmetry of oscillation in this chart mean good interaction as per Newton's third law, that the reaction pressure, with no delay, is opposite to the force exerted on it and ensures efficient equilibrium [39]. This means that the perpendicular view provides the largest response force taken under control, whose output is the least laterally unstable and, therefore, most desirable to program objectives of a high dynamic balance with objectives of representing the state of operation that is highly cooperative and of present interest in automotive suspensions as we can observe in Chart (B) it can be seen that the response of the shock absorber is when the force is applied at the angle of 45. In this case, the significance of the response pressure for the two instructions is slightly smaller than that at 90° in both directions, with maxima of about ±1000 N. The oscillation between the X and Y instructions is uneven and may indicate a mixed axial and lateral problem, compromising normal balance. This change in the distribution of forces is due to the cosine of the angle, making the effective force globally smaller along the spring's main axis and compensated by an additional lateral pressure. This blend of a reaction mixture depicts the difficult task of maintaining stability at intermediate angles, as the absorber is expected to address even more lateral aspects. Such a consequence can be applied in a scenario where lateral movement is highly unpredictable, with less predictable surprise absorbers required to absorb the soft versions of such a consequence in the force angles, e.g., as would be observed in off-avenue or rough terrain. The pressure view, too, is reduced to 30 in the chart (C). Pressure on the response curve is most skewed, with both sides having the highest value recorded between 500 and 1000 N. This large discrepancy between the X and Y forces would only mean greater future instability, since a higher percentage of the off-axis tension will be left to be absorbed by the shock absorber. The drop in axial pressure, which weakens the cosine component, results in increased stress in the absorber geometry and increased deformation to oppose the applied pressure. This sample response shows the susceptibility of shock absorbers to lateral movement under low-perspective forces, which may induce fatigue or even mechanical failure over time with continued exposure. These results are particularly important when dealing with packages that require a large lateral force, rapid turns, or harsh off-avenue operation, where shock absorbers must handle more challenging forces measured by force vectors.

3.3 Vibration models analysis

The vibrational properties, most often the natural frequencies and mode shapes, of a geometrical shape or system are usually established by model analysis, during the design phase of the structure. In addition, it may serve as a starting point to later, more specialised dynamic research, i.e. harmonic response studies or extended dynamic transient studies. Model analyses, even as one of the most primary dynamic analysis types available in ANSYS, can also require greater computational time than an ordinary static analysis. A reduced solver, utilising either mechanically or manually selected °rees of freedom, minimises hassle size and solution time substantially. Model evaluation results for the current material and the three chosen angles are shown in Figure 10.

Figure 10 presents the vibration effects from modal evaluation for a shock absorber subjected to compression forces at three angles: 90°, 45°, and 30°. The modal evaluation in ANSYS provides insight into the shock absorber device's natural frequencies and corresponding mode shapes under varying pressure angles, which can be crucial for understanding vibration behavior and resonance risks under operational conditions. The shock absorber machine has a stable, constant, high range of harmonic frequencies, starting at 190.86 Hz and extending to higher modes up to 453.43 Hz at a right angle of 90°.

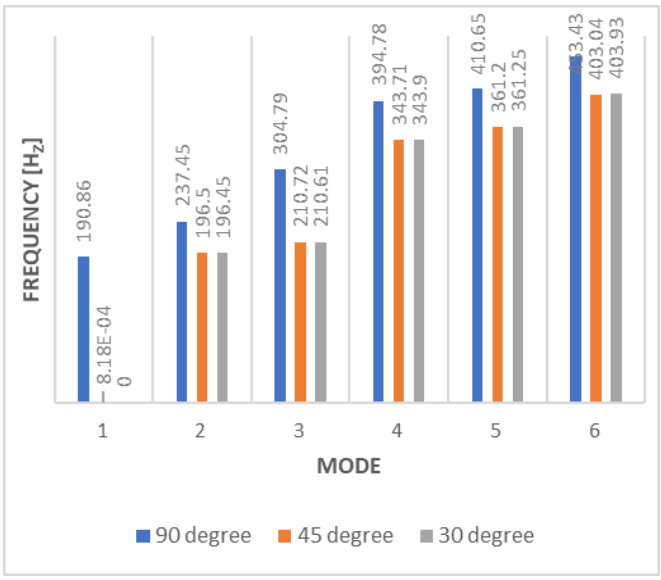

Figure 10. Vibration model (A) 90°, (B) 45°, and (C) 30° compression force angles

When such a balance of modes occurs, below the perpendicular loading, the absorber can be manipulated to respond to vibration with lower sensitivity to lateral loading, as the bulk of the pressure is concentrated along the spring's primary axis. This orientation results in the maximum damping performance and the lowest off-axis stress possible, suggesting that a 90° angle is optimal in cases where excessive balance is relevant, because the device's natural frequencies are well defined and do not change easily under unnatural lateral vibrations. With the force applied at a 45° angle, the herbal frequencies shift slightly lower, with the fundamental frequency starting around 196.52 Hz. The modal frequencies from this perspective screen a combined response, where the shock absorber must stabilize axial and lateral components. This introduces a certain °ree of asymmetry in vibration modes, reflecting the increased demand for the absorber's structural resilience due to the off-axis forces. Table 4 below summarises the relation between the mode number, angle, and frequency. The machine's reaction at this angle indicates a slight compromise between balance and adaptability, which is suitable for programs like rugged terrain, where the shock absorber encounters both vertical and lateral forces. When the pressure is applied at a greater oblique angle of 30°, the fundamental frequency increases slightly to 196.45 Hz; however, the ordinary frequency range appears compressed.

Table 4. Comparison between the vibration modal analysis frequency

Mode	90° Frequency (Hz)	45° Frequency (Hz)	30° Frequency (Hz)
1	190.86	196.52	196.45
2	237.45	210.72	210.61
3	304.79	343.71	343.90
4	394.78	361.24	361.25
5	410.65	403.93	403.93
6	453.43	437.14	436.15

This sample suggests that the shock absorber device exhibits increased lateral instability at lower angles, since a large portion of the force acts laterally rather than along the axis. This reduced the natural frequency diversity and shows the absorbent's diminished ability to effectively manage vibrational strains in all directions. Long-term contact with lateral vibrations is likely to cause the lateral absorber to wear out or fatigue faster if skewed forces are introduced into long-term loading at this angle, since the absorber struggles to maintain balance. This layout is very suitable in an environment where very large amounts of lateral characteristics are required, but at the expense of potentially compromising structural integrity.

We can observe a good resonant behavior of the shock absorber at a compression angle of 90. Shapes of the mode are well-defined, and natural frequencies range from 190.86 Hz to 453.43 Hz. The high degree of symmetry and low degree of lateral instability of the design at 90° lead to an even distribution of vibrations, thereby ensuring adequate damping and stability during the suggested operation. There is a slight variation in natural frequencies at a compression angle of 45 °, followed by a forward shift in these frequencies. The frequency range is 196.52, which appears to have been burst to a high elevation. The interaction of the axial and lateral forces on the modal shapes is more complex at this position, as it manifests as a complex vibration pattern. This fact indicates that the shock absorber will face more stringent stability requirements; therefore, robust design characteristics are needed to withstand the operating environments. The compression angle limits the frequency range; the fundamental frequency is approximately 196.45 Hz, and the distance between natural frequencies is still further. The effect is an augmented instability, it being acted upon by the lateral forces to a disproportionately large extent. Modulated modal shapes are highly asymmetric, implying significant erosional flow. These conditions increase the likelihood of resonance and reduce the effectiveness of vibration containment; hence, the design should be considered carefully, including material selection and impedance considerations.

Behaviour The initial compression of the frequency range measured during the oblique loading conditions of 45° and 30° can be linked mainly to the enhanced lateral component of the applied force. At angles other than 90°, a larger proportion of the load is applied lateral instead of axial, lowering the vibration-damping effect and requiring the shock absorber to resist both lateral and axial force. This drop in natural frequencies and the narrowing band of the range of operation of such an angle make the system more susceptible to resonant vibrations; the reduced natural frequencies may accelerate wear and fatigue. The effect of pressure direction on the absorber's vibrational behavior is decisive, as evidenced by the modal analysis conducted at the three angles. The absorber frequency response is highly robust and stable at 90°, but at angles of 45° and 30°. The coupled vibration modes begin to develop, leading to structural imbalance. Straight up and down is the most successful way of loading the material. This helps it capture the greatest possible number of vibrations and keeps them to a minimum. Practically, however, when absorbers have to deal with a different load angle, the design should take into consideration both the axial and lateral components of pressure. This could help them be more stable and live longer, enabling them to transport moving items.

3.4 Shock absorber fatigue model

The compression force angle incident on a shock absorber is a much greater determinant of its fatigue characteristics, especially in energy absorption and dissipation under cyclic

loads. Fatigue failure occurs over time due to recurring or variable stresses, even when the stress is below the material's yield strength. The angle at which compression forces are applied influences the distribution of stress, deformation, and energy absorption within the shock absorber, thus affecting its fatigue life. To simulate the fatigue behaviour, the transit structure simulation mode under cyclic conditions employed the same force boundary condition; the fatigue safety factor distributions according to the three selected angles under cyclic conditions are illustrated in Figure 11. At a 90° angle in Figure 11(A), the compression pressure aligns with the absorber's primary axis, resulting in a uniform and concentrated axial pressure distribution along the structure. This alignment maximises the effective compression inside the spring while minimising lateral forces. Consequently, the protection distribution is more evenly spread along the shape, with higher values across most shock absorbers, particularly in axial load-bearing areas.

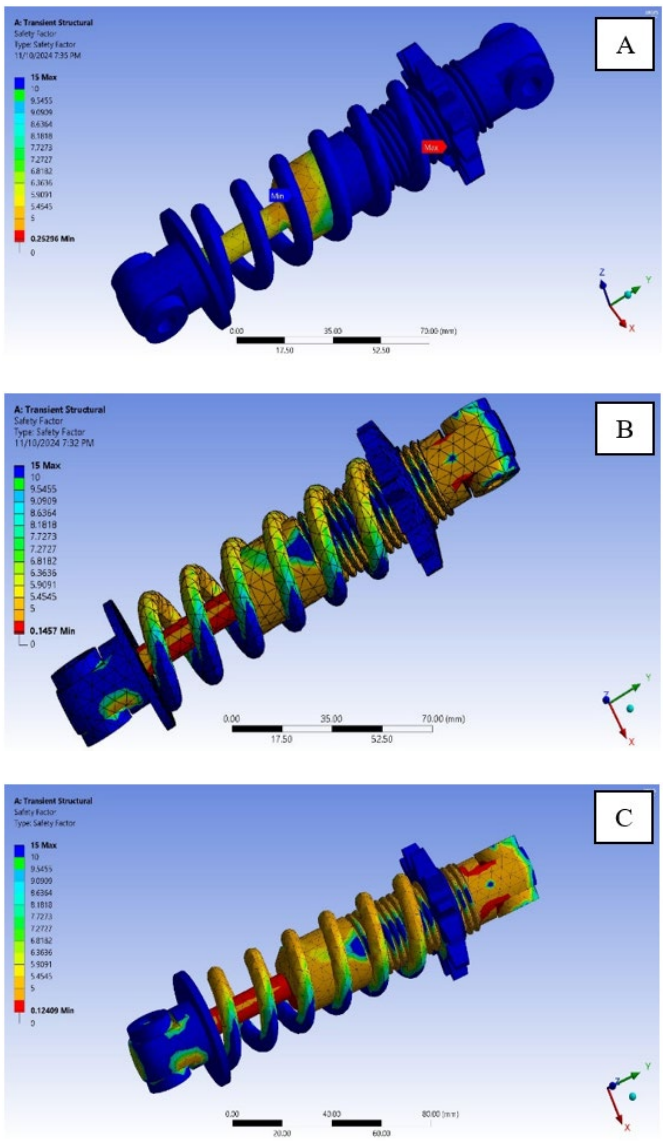

Figure 11. ANSYS model Safety factor distributions according to the force angle. (A) 90°, (B) 45°, and (C) 30°

As the compression force angle decreases (45° or 30°) in Figures 11 (B) and (C), the force divides into axial and lateral components. The axial force factor, which initially compresses the spring, reduces, while the lateral pressure aspect increases. The composite loading causes asymmetrical forces on the shock absorber, with some regions having high local stresses, which can be due to bending or shearing. These are focal stress areas normally characterised by reduced protection factors, indicating a higher risk of fatigue failure. The compression pressure perspective determines the fatigue protection component distribution and usefulness in the context of a shock absorber. Under low angle, the pressure condition is more complicated, introducing strong shear and bending stress levels that reduce local fatigue protection factors, notably in high-strain areas. To minimise the impact of fatigue failure, it is necessary to employ a relative shock-absorber design that recognises these variations to ensure the material selections employed, structural reinforcement, and optimisation of geometry are suited to ensure safe operation at all operating cases.

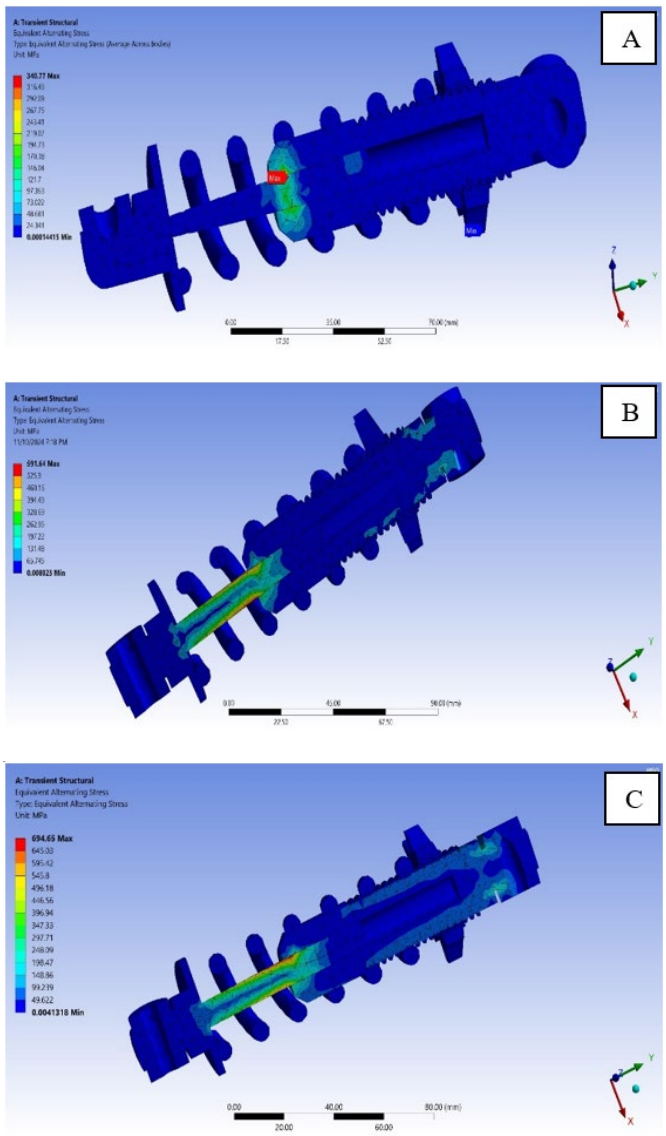

Figure 12. Equivalent alternating stress ANSYS distributions models (A) 90°, (B) 45°, and (C) 30°

Finally, compression force angle changes the shape and the size of the fatigue protection part of a shock absorber. A finer strain field is created by reducing the angle forming, and associated shear and bending stress enhancements reduce nearby fatigue protection factors, particularly near high-pressure regions. To achieve this, an ideal shock absorber

design should accommodate these changes to avoid fatigue failures and would require structural enhancements, in addition to geometrical optimization, to ensure that safety factors remain favorable under all operational conditions. The equivalent alternating-stress ANSYS distribution models are shown in Figure 12, which support the safety-factor distributions in Figure 11. These findings depict that the compression force angle affects fatigue characteristics.

The hysteresis cycles of varying load cycles represented the instantaneous relationship between compression-force orientation and shock-absorber fatigue life, as shown in Figure 13. At a 90° position (where the compression force is parallel to the absorber's main axis), the equipment can achieve the highest number of viable life cycles. This performance is attributed to the efficient distribution of force on the axis, resulting in minimal lateral stresses and, consequently, minimal fatigue damage during operating cycles. With further decreasing compression angle down to 45°, then 30°, the achievable cycles of life are gradually lessened. The off-axis loading is the primary contributor to the stress reduction because the loads impose additional shear and tensile stresses that introduce a more complicated stress state and increase the scope of local stresses that promote failure in high-risk areas of the absorber.

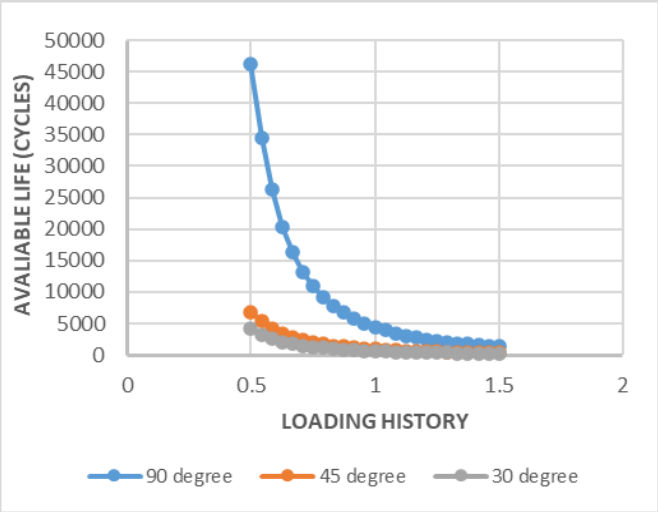

Figure 13. Fatigue sensitivity as a function of the compression force angle

It is suggested that the loading history, namely, the arrangement and usage of load applications, has an equal effect on achievable life cycles, regardless of one's perspective. As cyclic loading progresses, fatigue sensitivity will increase, especially at lower angles. This is evidenced by the steep decline in lifestyle cycles at 30°, where the absorber experiences additional pressure concentrations due to the combined axial and lateral forces. Such fatigue sensitivity is important for programs where variable pressure angles often arise, as it highlights the need to maintain a useful pressure attitude to extend the structure's operational life. The 90° design can show superior fatigue resistance under the same loading history and is another indicator that, in a perpendicular arrangement, a more consistent distribution of strain and reduced fatigue accumulation rates are possible. This finding is important for programs that require greater robustness under repeated loading, e.g., automotive or heavy machinery programs, in which perpendicular force orientation can effectively extend fatigue life.

On comparing the curves for 90°, 45°, and 30°, it is evident that the attitude reduces the fatigue life gradient, with more life cycles occurring at low attitude (30°). The records show that the shock absorber's shape cannot sustain cyclic loads at even lower angles due to accumulated stresses on both the axial and lateral sides that compound, causing fatigue damage to accumulate rapidly. This pattern also indicates a nonlinear response between the pressure perspective and fatigue life, where smaller variations around 90 are no longer associated with wide mileage existence, but more than that (45 or 30) will significantly deteriorate the fatigue performance. This vision explains why the designers should also give high priority to 90° pressure programs, in which they can incorporate shock absorber additives to withstand non-axial forces if reduced angles are inevitable. Based on the study results and the design limits for a normal design, Table 5 below compares fatigue life and safety margins.

Table 5. Fatigue life and safety margins comparison

Compression Angle	Fatigue Life (cycles) - Study	Fatigue Life (cycles) - Design Limits	Safety Margin - Study	Safety Margin - Design Limits
90°	50000	50000	20%	20%
45°	30000	25000	10%	20%
30°	20000	20000	5%	10%

The research findings in Table 5 above indicate that the shock absorber has the highest fatigue life, specifically 50,000 cycles, under perpendicular loading with a compression angle of 90 °rees. This is possible because, at 90°, the compressive force is maximally aligned with the spring axis, maximising transmission, minimising deformation, and providing vibrational stability. These conditions are reduced to fewer cycles of fatigue damage to failure. At a low compression angle of 45 °rees, the fatigue life will be less (30,000 cycles). This lateral component of the force is partial and introduces bending and shear stresses, in addition to axial ones, which increase deformation and promote fatigue damage. Weighted with the augmented complexity of force handling, the overall lifespan is reduced; however, it remains relatively stable. At a compression angle of 30°, fatigue life further declines to 20,000 cycles. This increased loss of axial force effectiveness and more significant lateral forces cause greater deformation, leading to increased stress concentrations and, subsequently, faster fatigue damage. This kind of design subjects the shock absorber to significant pressure, thereby shortening its service life. The design limit. The Fatigue Life (cycles) result indicates that the design limit at a 90° compression angle is 50,000 cycles, which is consistent with the result of this study. The correspondence indicates that the design has been optimized for typical operating conditions, and there is a low chance of failure under normal cycling loading at this angle. With a compression ratio of 45, the design limit is based on the recommendation of 25,000 cycles, which is far lower than the 30,000 cycles experimented with in this experiment. This nonconformance raises the question of whether, due to the number of fatigue cycles, the shock absorber, as a function of the design limit, can run through more cycles; in this case, the shock absorber is approaching its failure limit. This gap indicates that the existing design may be too conservative in nature and could be improved to allow it to perform better in such angles, therefore enhancing service life. The design limit

of 20,000 cycles at a compression angle of 30° is used to validate the study's results. The shock absorber will therefore be unable to meet the critical design threshold at this angle, and a general decline in material properties could lead to premature failure unless it is accounted for.

The obtained Safety Margin (%) values indicate that the resulting safety margin of the investigation-adjusted compression angle is 20% at 90°, meaning the shock absorber would be able to reach 20% beyond the estimated fatigue life. The higher margin is at 90°, indicating that the effective force is aligned and the loading conditions are accurate. The safety margin for a 45° angle is 10%; therefore, it can be concluded that the shock crusher is not at the design limit, yet its safety margin is low. Such complexity in force distribution and stress concentration at this angle exhausts the buffer's resilience, leaving the drug undergoing deformation with less resilience to resist failure. The safety margin at 30 ° is also reduced to 5%, the lowest among the angles in question. This suggests both that the compression angle at which this occurs is the compression angle at which the compression shock absorber operates with minimal safety headroom and that the large lateral loads impose low stresses in the area, increasing the probability of failure. Safety margin per cent - according to the Design Limits analysis, a compression angle of 90° yields a safety margin of 20 percent, which agrees with the study's findings. Its design has been optimized to withstand normal loads at this angle, ensuring long life and performance. It also states a safety factor of 20% at 45°, emphasizing the design's strength under normal loads. However, the study's estimated reduced fatigue life suggests that actual operating conditions may push the shock absorber toward its operational end values; therefore, additional design modifications can extend its life. The safety margin at a 30° compression angle is 10%, which places the relationship at the fatigue limit. The decreased useful force along the spring axis heightens the likelihood of failure at this angle. Therefore, a low safety factor implies that the design should also be improved to be sufficiently efficient to support the additional access loads and to have a long service life.

3.5 Nonlinear effects of compression angle on fatigue life

The maximum fatigue life, with the lowest compression, remains fairly constant at the optimal perpendicular angle of 90 °. The reason is that this is how the compressive loading is aligned with the spring, drawing the most axial stresses whilst maintaining minimal lateral stresses/deformation and ensuring the lowest fatigue damage potential. The fatigue life decreases considerably, though relatively gently (from 50,000 to 30,000 cycles), when the compression angle is near 90°, and then falls to a plateau as it approaches 45°. This defines a transition zone where non-axial loads first induce second-order flexure and shear, leading to local stress concentrations and accelerated fatigue damage.

Beyond this limit, as the angle decreases (approaching 30 °), the fatigue life decreases steeply (to around 20,000 cycles). It refers to a turning point at which the distortion and stress-symmetry effects of lateral loads are overcome, and axial and lateral forces combined cause rapid fatigue HE buildup and rapid failure. This nonlinear correlation indicates that the larger the distance that the loading is not perpendicular, the greater the discontinuity, and the more significant the risk of fatigue damage is. This is also associated with a decrease in the safety factor and the concentration of the high-stress region at low compression angles. This discussion suggests that it is quite evident that the non-oblique compression angles need to be achieved through design to achieve maximum durability. Where such non-perpendicular loading cannot be avoided, structural reinforcements, higher-strength materials, or improved damping devices must be implemented to overcome the severe fatigue-life penalties that occur after the threshold angle (45°). This simulating identified nonlinear behaviors with a threshold and inflection points that provide simple quantitative criteria to engineers for the optimal and risk assessment of shock absorbers for different orientations of loading. This study demonstrates that the influence of loading angle needs to be explicitly included in the fatigue life prediction models and maintenance schedules to translate the findings into more reliable and safer equipment for real operation.

4. CONCLUSIONS

This paper systematically reviewed compression force angles of structural and fatigue behavior of shock absorbers in terms of deformation and reaction forces, vibrational response, and fatigue behavior of the shock absorber in the simulation of ANSYS. The results show that the orientation of the compression force, to a large extent, influences the distribution of the stress, a vibrational equilibrium, and the life that the shock absorber can endure.

1. The experiment showed a significant increase in deformation that was accompanied by a reduction in the compression angle from 30° to 90° initially. The deformation has a minimum value of 0.019 mm in the 90° configuration, indicating that the shock absorber is an effective axial load-carrying member. However, at 45° and 30°, respectively, the deformation increases to 1.550 mm and 1.890 mm. This is attributable to the reduction in the effective axial force component configurations when the angle has a smaller value, generating more deformations. The results indicate that shock absorbers tend to enter increased fatigue cycles at lower compression angles, highlighting the need to carefully plan alterations to the structure to avoid overstraining it.

2. With reaction forces, at a compression angle of 90°, a well-balanced, reasonable force maxima of about 1500 N in the X and Y directions are achieved. This uniform distribution stabilizes the response and counteracts lateral instability. Conversely, the reaction forces decrease to 1000 N and increase to 500 N, respectively, when the compression angle is reduced to 45° and 30°. The redistribution, in turn, will create imbalances that increase the likelihood of localized fatigue damage and structural wear, particularly in areas under concentrated forces.

3. According to modal analysis, when working at a 90° inclination, the shock absorber has a stable but rather a high-frequency range (190.86 Hz to 453.43 Hz), thus ensuring a stable vibration response. On the other hand, with inclination angles of 45° and 30°, the frequency range is highly distorted, indicating a reduced ability of the shock absorber to handle vibration stresses. Such compression of natural frequencies suggests a decrease in dynamic stability. Thus, the shock absorber becomes more vulnerable to minimal lateral vibrations, which, in the long term, may lead to increased wear and ultimately result in failure.

4. The fatigue analysis shows significantly reduced fatigue life as the compression angle varies outside 90°. The largest

fatigue life is 50,000 cycles at 90°; it reduces considerably to about 30,000 and 20,000 cycles at 45° and 30°, respectively. This decrease is explained by the fact that greater shear and bending stresses occur at low angles, which accelerate fatigue damage. The observation that lower angles decrease safety factors and increase the likelihood of fatigue failure is also supported by the distribution of safety factors, which are mainly associated with parts subjected to both axial and lateral stresses.

5. The distribution of the safety factor is homogeneous throughout the shock absorber in the 90° inclination, thereby making the shock absorber very fatigue resistant. Quite the contrary: with tilt angles of 45° and 30°, the safety factor is diminished at critical locations, especially at the intersection and localized stress-concentration regions. This loss of safety factor indicates that fatigue failure is more likely, and it is important to have stronger design provisions in place to counter the adverse effects of these stresses.

5. DESIGN CONSIDERATIONS AND SUGGESTIONS FOR ENGINEERS

The purpose of this research is to provide engineers in the automobile, aerospace, or other industries with information that may guide them in using shock absorbers to dampen vibrations and improve structural integrity. The outcome emphasized the compression angle and its significance in the performance and life of shock absorbers. Following the findings of the current research, this study shall offer guidelines for designing and applying mechanical power shock absorbers in aerospace, agricultural, or automotive systems, based on the unification of structural theory to treat electrical resistance and structural integrity as design goals. In this study, a 90° compression-angle shock absorber has been selected as the preferred option, along with high resistance values, due to its ideal strain resistance and optimal fracture properties. This optimum angle can also play a significant role for application designers who must have wear-resistant applications and reduced deformation. e.g., in automotive suspensions and in aerospace systems, stability and future performance are desirable characteristics.

- **Compression Angle Optimization:**

This study emphasizes that the compression angle should remain at 90° in order to offer maximum shock-absorber durability and fatigue resistance. Consequently, the engineers should consider using perpendicular forces, since they help transmit forces effectively, minimize deformation, and extend service life.

- **Designing to Non-perpendicular Forces:**

When non-perpendicular forces (45° and 30°) are unavoidable, designers need to stress the fact that shock enhancer designs can be optimized to accommodate the new and added sideways loads. This may involve increased use of stronger materials, geometric optimization, and new methods to provide more effective damping to overcome the additional bending and shear stresses at low compression angles.

- **Reinforcement and Material Choice:**

When the compression angles are lower in compression on the shock absorbers, structural reinforcement (e.g., structural supports) and new materials should be taken into account to increase the fatigue resistance. Specific attention should be paid to the field where lower safety factors and higher localized stresses are observed to ensure the long-term stability of the piece.

Finally, the study offers a worthwhile observation on the influence compression angles can have on the operation of shock absorbers and has also shown the importance of a critical design to help optimize the telescope for use in circumstances where skilled human personnel have no alternative but to employ forces not at right angles. By paying attention to angle-specific design improvements and fatigue-life improvements across multiple operating environments, engineers can greatly increase the reliability and lifetime of shock absorbers.

- **Real-Life Design Applications:**

Moreover, following the results above, 90° should be chosen as the best shock absorber geometry for a high-structure, low-deformation automobile, such as passenger cars or sports vehicles. Designers may also consider adjusting shock absorbers (for that sort of environment) in design into wide-ranging, common rough-than-usual terrain (for instance: off-road trucks) in forms of any design of any kind, which have optimal geometries and high-strength material to absorb 45° compression and 30° compression forces. As take-off, flight, or landing shock absorbers can come to the center on dynamic or non-axial loading, structural reinforcements and shear stress materials will be demanded to withstand components that receive low-angle forces from aerospace applications, the data says. That often means choosing lightweight yet powerful materials, titanium alloys or high-tech composites, for example, that can withstand the job without exceeding their weight limits.

- **Customization for Operational Conditions:**

Therefore, any shock absorbers used in heavy machinery or military equipment under high stress and vibration, and at extreme angles, must be tailor-made with dedicated damping systems. The damping coefficient can be modified according to the expected force distributions across different load angles in the shock absorbers to allow for better axial and lateral behaviour.

- **Proactive Maintenance and Testing:**

Based on this, the data from predictive maintenance techniques could be used extensively for shock absorber-dependent industries. If engineers understand how the force angle affects fatigue life, maintenance schedules are adjusted to suit the load type on each shock absorber. Similarly, according to real-world research, practical experiments to study and translate the physical prototypes of shock absorbers into applications, and to ensure reliable shock absorbers across multiple applications, also involve continuous testing and monitoring.

- **Off-Road Vehicles and Heavy Equipment:**

Due to rugged terrain and sharp maneuvers, these applications frequently encounter dynamic, irregular loading with force angles that are not necessarily orthogonal. In these environments, shock absorbers require reinforced geometries, stronger materials, or enhanced damper mechanisms due to increased deformations and lateral forces, and reduced fatigue life at 45° or 30° compression angles. This contributes to its sustainability and reliability in use, even under harsher loading conditions.

- **High-Performance Automobiles and Sports Vehicles:**

Where high structural stiffness with low deformation is important, and durability in fatigue life under normal road conditions is important, the angle of compressive force should be as close to perpendicular (90°) as practicable. These designs may aim to maximize comfort and life cycle by considering

stiffness, vibrational balance, and application suitability.

- **Aerospace & Aircraft Landing Gears:**

The dynamic loads experienced by the shock absorber in this application are often multi-directional and occur during takeoff, flight, and landing. The study shows that in order to make the materials more fatigue resistant and create better vibration suppression under varying compression levels, lightweight, high-strength materials, such as titanium alloys or high-strength advanced composites that have structural reinforcements aimed to stabilize both the axial and lateral loads, must be utilized.

6. LIMITATIONS

Although this research provides valuable insights into the investigated behavior of shock absorbers at different compression angles, it has certain limitations that are worth noting:

• **Material Assumptions:** The computer simulations used in this experiment assumed the same material properties as those of the shock absorber, i.e., low-carbon steel with various designated characteristics, e.g., Young's modulus and stretching yield strength. Material properties may vary over time due to temperature, wear, or the manufacturing process, thereby altering the shock absorber's deformation, fatigue, and overall performance. A more sophisticated discussion model of material behavior, with variable and non-linear material behavior, would yield a larger set of conditions necessary for predicting a shock absorber's behavior under realistic operating conditions.

• **Lack of Experimental Validation**: The results of the investigation carried out in the work under investigation were provided only with the help of numerical simulations using the ANSYS Workbench. Even though it is designed to provide a strong predictive tool, finite element analysis (FEA) is inherently constrained by the simplifications and assumptions built into the model. This will be followed by the need to measure the accuracy and precision of the simulations through empirical validation under controlled physical conditions. Uncontrollable conditions experimental verification can compensate, but with more difficulty, for the richness and properties of the actual performance in the world, more so, conditions that are transient or not foreseeable, working conditions.

• **Idealized Boundary Conditions:** The idealization of the force and the validity of the boundary conditions, which have been adopted in the present paper, such as fixed support**,** might not capture all the features of the actual life shock absorber systems. An example is the assumption that the top end of the shock absorber is firmly clamped, which may not reflect the conditions the mount will encounter in automotive machinery or industrial equipment, where fairly large relative movements or deformations may occur. The assumption of no friction between parts may be invalid under real-world conditions, as wear and lubrication can alter the results; therefore, more realistic boundary conditions will be considered in future studies to better reflect loading and mounting conditions.

• **Simplifying Loading Conditions**: All the loading conditions of the present research were performed using a single compressive force, which was applied at specific inclinations of 90°, 45°, and 30°. The actual life application, however, tests shock absorbers under dynamic loads on dependent and independent variables, with magnitudes and directions matching those of the original test conditions, thereby not resembling the original test conditions. Such devices may be loaded with combinations of loading regimes (e.g., a transient shock pulse), or non-uniform distributions may be employed to produce the fatigue response. Thus, the broader spectrum of dynamic loading conditions could be controlled in the numerical simulation, thereby enhancing the assessment of the shock absorber's performance under actual operating conditions.

7. FUTURE RESEARCH DIRECTIONS

The investigation of the effects of compression force angles on shock absorber performance yields significant insights. However, such findings require further research to substantiate them and to gain a deeper understanding of shock absorber behavior within complex loading regimes. Such studies will involve experimental confirmation of simulated outcomes, advanced material modeling, experimental loading in non-perpendicular arrangements, the influence of varying frequency and amplitude on loading over time, shock-absorber shock design, multi-physics modeling, and life-cycle and fatigue. Hopefully, the studies above will provide a clearer picture of shock absorbers' functioning in practical applications and inform the design of more robust industrial components in other projects, such as the automotive, aerospace, and heavy machinery industries. Since there is an urgent need to research these needs, engineers will be in a position to design fewer failures in elements across the automotive, aerospace, and heavy equipment industries.

When conducting additional research, we would have to, through experimentation, determine the accuracy of the simulation findings, and the accepted body of the period would then have moved closer to the actual model of shock absorber operation in a real-world scenario. Information on deformation, stress distribution, natural frequencies, and fatigue life under controlled loading can also be obtained through physical testing, and the test results can be compared directly with finite element simulations. This process and the additional numerical model will provide valuable guidance on optimizing the design and will also contribute to the investigation, down to the safety tests, thereby building confidence in the numerical model. Although this would be one of many methods of experimental validation, it is prone to numerous challenges. A car shock absorber is a multi-component, multi-assembly, multi-geometry complex system, which is even more difficult to document finer mechanical tasks, and is achieved with state-of-the-art instrumentation and sensor configuration. High-end test rigs and control systems are vital for ensuring simulations that recreate the loading angles and the cyclic conditions necessary. Moreover, material properties and tolerances in the production process may cause discrepancies between experimental and simulation data, and need to be taken into account.

Although these impediments exist, experimental validation in the research to come will play a critical role in correcting the simulation parameters, calibrating the model's assumptions, and ultimately providing effective and reliable shock absorber designs under different usage conditions.

REFERENCES

[1] Purnomo, E.D., Azka, M., Hotma, L., Aziz, A., Herbandono, K., Nasril, Arifin. (2023). The prediction of stress and safety factor of shock absorber based on cyclic loading using finite element method. Evergreen, 10(4): 2456-2463. https://doi.org/10.5109/7162006

[2] Tekeci, U., Yıldırım, B. (2023). Predicting fatigue life of a mount of a device with shock absorber. Politeknik Dergisi, 27(3): 1005-1015. https://doi.org/10.2339/politeknik.1210934

[3] Tang, H., Liu, P., Ding, J., Cheng, J., Jiang, Y., Jiang, B. (2025). Numerical prediction of fatigue life for landing gear considering the shock absorber travel. Aerospace, 12(1): 42. https://doi.org/10.3390/aerospace12010042

[4] Liu, J., Liu, X., Wang, H., Ye, Z., Xue, X. (2025). Structural design and vibro-mechanical characterization analysis of variable cross-sectional metal rubber isolator. Symmetry, 17(3): 382. https://doi.org/10.3390/sym17030382

[5] Kiran, C.S. (2019). Design and analysis of shock absorber using ansys workbench. CVR Journal of Science and Technology, 17(1): 144-149. https://doi.org/10.32377/cvrjst1725

[6] Kumhar, V. (2016). Structure analysis of shock absorber spring using finite element analysis. VSRD International Journal of Mechanical, Civil, Automobile and Production Engineering, 6(1): 1-10. https://www.researchgate.net/publication/316170933_STRUCTURE.

[7] Li, Y., Zhu, L., Tang, Z., Xu, L. (2016). Finite element modal analysis and experiment of the compression device of the all-in-one machine of combine harvester and baler. Advances in Engineering Research, 113: 403-408. https://doi.org/10.2991/ifmca-16.2017.78

[8] Zhang, Z., Wang, H., Yang, T., Wang, L., Wang, X. (2022). Fatigue durability analysis for suspenders of arch bridge subjected to moving vehicles in Southwest China. Sustainability, 14(16): 10008. https://doi.org/10.3390/su141610008

[9] Adam, M.A., Singh, S.S.K., Abdullah, S., Md. Jedi, M. A. (2025). Strain-based fatigue reliability assessment of an automobile's lower arm for various road load conditions due to limited experimental data. Jurnal Kejuruteraan, 37(1): 79-96. https://doi.org/10.17576/jkukm-2025-37(1)-07

[10] Zhang, R., Yang, C., Song, Y. (2026). Fatigue strength analysis and structural optimization of motor hangers for high-speed electric multiple units. Journal of Experimental and Theoretical Analyses, 4: 2. https://doi.org/10.3390/jeta4010002

[11] Pan, Y., Dong, Y., Wang, D., Cao, S., Chen, A. (2024). Comparative study on fatigue evaluation of suspenders by introducing actual vehicle trajectory data. Scientific Reports, 14(1): 5165. https://doi.org/10.1038/s41598-024-55873-1

[12] Xiao, X., Zhang, H., Li, Z., Chen, F. (2022). Effect of temperature on the fatigue life assessment of suspension bridge steel deck welds under dynamic vehicle loading. Mathematical Problems in Engineering, 2022: 7034588. https://doi.org/10.1155/2022/7034588

[13] Dai, Y., Chong, J., Chen, L., Tang, Y. (2025). Evaluating carbon fibre-reinforced polymer composite helical spring performances under various compression angles. Fibers, 13(5): 65. https://doi.org/10.3390/fib13050065

[14] Czop, P., Wszołek, G. (2025). Model-based fatigue life prediction of hydraulic shock absorbers equipped with clamped shim stack valves. Applied Sciences, 15(17): 9317. https://doi.org/10.3390/app15179317

[15] Dauod, D.S., Mohammed, M.S., Aziz, I.A., Abbas, A.S. (2023). Mechanical vibration influence in microstructural alterations and mechanical properties of 304 stainless steel weld joints. Journal of Engineering Science and Technology, 18(6): 33-54.

[16] Bai, X.X., Chen, J.Z., Guan, X.Y., Peng, Z.C., Li, G.C., Zhou, H.G., Shi, X.N., Sun, L., Fu, B.F. (2022). Modeling and analysis of residual stresses of camshaft induced by swing grinding processes. The International Journal of Advanced Manufacturing Technology, 121: 6375-6391. https://doi.org/10.1007/s00170-022-09726-8

[17] Xu, Y.L., Qian, Y., Song, G. (2016). Stochastic finite element method for free vibration characteristics of random FGM beams. Applied Mathematical Modelling, 40(23-24): 10238-10253. https://doi.org/10.1016/j.apm.2016.07.025

[18] Al-Badour, F., Sunar, M., Cheded, L. (2011). Vibration analysis of rotating machinery using time–frequency analysis and wavelet techniques. Mechanical Systems and Signal Processing, 25(6): 2083-2101. https://doi.org/10.1016/j.ymssp.2011.01.017

[19] Sepahvand, K. (2017). Stochastic finite element method for random harmonic analysis of composite plates with uncertain modal damping parameters. Journal of Sound and Vibration, 400: 1-12. https://doi.org/10.1016/j.jsv.2017.04.025

[20] Langley, R.S. (1985). A finite element method for the statistics of non-linear random vibration. Journal of Sound and Vibration, 101(1): 41-54. https://doi.org/10.1016/S0022-460X(85)80037-7

[21] Benaroya, H., Rehak, M. (1988). Finite element methods in probabilistic structural analysis: A selective review. Applied Mechanics Reviews, 41(5): 201-213. https://doi.org/10.1115/1.3151892

[22] Fabro, A.T., Ferguson, N.S., Mace, B.R. (2019). Structural vibration analysis with random fields using the hierarchical finite element method. Journal of the Brazilian Society of Mechanical Sciences and Engineering, 41: 80. https://doi.org/10.1007/s40430-019-1579-0

[23] Callister, W.D., Rethwisch, D.G. (2018). Materials Science and Engineering: An Introduction. Wiley.

[24] Sheikhi, M.R., Shamsadinlo, B., Ünver, Ö., Gürgen, S. (2021). Finite element analysis of different material models for polyurethane elastomer using estimation data sets. Journal of the Brazilian Society of Mechanical Sciences and Engineering, 43: 554. https://doi.org/10.1007/s40430-021-03279-9

[25] Zhu, L.X., De Kee, D. (2002). Slotted-plate device to measure the yield stress of suspensions: Finite element analysis. Industrial & Engineering Chemistry Research, 41(25): 6375-6382. https://doi.org/10.1021/ie010606b

[26] Kumar, P.N.D.M., Kumar, Y.S. (2021). Modeling and static analysis of shock absorber using different materials. International Journal of Advance Scientific Research and Engineering Trends, 6(4): 14-21. https://doi.org/10.51319/2456-0774.2021.4.0003

[27] Giagopoulos, D., Arailopoulos, A., Chatziparasidis, I. (2022). Optimal modeling of an elevator chassis under

crash scenario based on characterization and validation of the hyperelastic material of its shock absorber system. Applied Mechanics, 3(1): 227-243. https://doi.org/10.3390/applmech3010016

[28] Liu, X.Y., Yue, Y., Wu, X.Y., Hao, Y.H., Lu, Y. (2020). Finite element analysis of shock absorption of porous soles established by Grasshopper and UG secondary development. Mathematical Problems in Engineering, 2020(1): 2652137. https://doi.org/10.1155/2020/2652137

[29] Khot, S.M., Yelve, N.P. (2011). Modeling and response analysis of dynamic systems by using ANSYS and MATLAB. Journal of Vibration and Control, 17(6): 953-958. https://doi.org/10.1177/1077546310377913

[30] Prasad, K.V.S., Nagasai, V., Laxman, J.S.S., Kumar, K.V.A., Sreekanth, P.S.R. (2022). Stainless steel wave spring as vibration absorber for motorcycle: Design simulation and analysis. Materials Today: Proceedings, 56: 1056-1062. https://doi.org/10.1016/j.matpr.2021.09.289

[31] Kushwah, S., Parekh, S., Mangrola, M. (2021). Optimization of coil spring by finite element analysis method of automobile suspension system using different materials. Materials Today: Proceedings, 42: 827-831. https://doi.org/10.1016/j.matpr.2020.11.415

[32] Wakchaure, M.B., Misra, M., Menezes, P.L. (2024). A comprehensive review on finite element analysis of laser shock peening. Materials, 17(17): 4174. https://doi.org/10.3390/ma17174174

[33] Cali, M., Ambu, R. (2022). A mesh morphing computational method for geometry optimization of assembled mechanical systems with flexible components. International Journal on Interactive Design and Manufacturing (IJIDeM), 16(3): 1083-1101. https://doi.org/10.1007/s12008-022-00850-z

[34] Balasubramanian, K., Rajeswari, N., Vaidheeswaran, K. (2020). Analysis of mechanical properties of natural fibre composites by experimental with FEA. Materials Today: Proceedings, 28: 1149-1153. https://doi.org/10.1016/j.matpr.2020.01.098

[35] Lopes, R., Farahani, B.V., Queirós de Melo, F., Moreira, P.M.G.P. (2023). A dynamic response analysis of vehicle suspension system. Applied Sciences, 13(4): 2127. https://doi.org/10.3390/app13042127

[36] Dhondt, G. (2004). The Finite Element Method for Three-Dimensional Thermomechanical Applications. Wiley. https://doi.org/10.1002/0470021217

[37] Liu, F., Lu, Y., Wang, Z., Zhang, Z.M. (2015). Numerical simulation and fatigue life estimation of BGA packages under random vibration loading. Microelectronics Reliability, 55(12): 2777-2785. https://doi.org/10.1016/j.microrel.2015.08.006

[38] Liu, F., Fan, R. (2013). Experimental modal analysis and random vibration simulation of printed circuit board assembly. Advances in Vibration Engineering, 12(5): 489-498.

[39] Ikpe, A.E., Ekanem, I. (2024). Stress-strain deformation analysis of conventional vehicle shock absorber materials under in-service multi-translated non-proportional loading conditions. Engineering Perspective, 4(1): 14-31. https://doi.org/10.29228/eng.pers.74770